Published in final edited form as:
Nat Neurosci. 2007 March ; 10(3): 348–354.

Dual functions of mammalian olfactory sensory neurons as odor detectors and mechanical sensors

Xavier Grosmaitre[1], **Lindsey C Santarelli**[1], **Jie Tan**[2], **Minmin Luo**[2], and **Minghong Ma**[1]

1 *Department of Neuroscience, University of Pennsylvania School of Medicine, 215 Stemmler Hall, 3450 Hamilton Walk, Philadelphia, Pennsylvania 19104, USA*

2 *National Institute of Biological Sciences, No. 7 Science Park Road, Beijing 102206, China*

Abstract

Most sensory systems are primarily specialized to detect one sensory modality. Here we report that olfactory sensory neurons (OSNs) in the mammalian nose can detect two distinct modalities transmitted by chemical and mechanical stimuli. As revealed by patch-clamp recordings, many OSNs respond not only to odorants, but also to mechanical stimuli delivered by pressure ejections of odor-free Ringer solution. The mechanical responses correlate directly with the pressure intensity and show several properties similar to those induced by odorants, including onset latency, reversal potential and adaptation to repeated stimulation. Blocking adenylyl cyclase or knocking out the cyclic nucleotide–gated channel CNGA2 eliminates the odorant and the mechanical responses, suggesting that both are mediated by a shared cAMP cascade. We further show that this mechanosensitivity enhances the firing frequency of individual neurons when they are weakly stimulated by odorants and most likely drives the rhythmic activity (theta oscillation) in the olfactory bulb to synchronize with respiration.

Receptor cells within each sensory system are specialized to detect a certain modality (for example, vision, hearing, touch, taste or smell) and to convert external stimuli into intracellular signals. Odor detection via the olfactory system relies on a large family of odorant receptors expressed in the olfactory sensory neurons (OSNs) within the neuroepithelium of the nose[1]. These odorant receptors initiate a cAMP pathway that enables olfactory signal transduction[2]. Binding of odor molecules to odorant receptors sequentially activates a specific G protein (Golf) and adenylyl cyclase type III (ACIII), which increases the intracellular cAMP level. Later opening of specific cyclic nucleotide–gated (CNG) channels by cAMP depolarizes the sensory neurons and triggers action potentials, which then permits odor information to reach the olfactory bulb in the brain.

In addition to processing the convergent odor inputs from numerous OSNs, the olfactory bulb shows rhythmic activity (theta-band oscillation) coupled with respiration even in the absence of odorants, suggesting that the bulb also receives airflow information[3–8]. The mechanism underlying the rhythmic activity is not fully understood, although both peripheral and centrifugal sources are implicated[6,9–12]. Nonetheless, air intake, especially in the form of

Correspondence should be addressed to M.M. (minghong@mail.med.upenn.edu.).

AUTHOR CONTRIBUTIONS

X.G. performed the recordings in the septal organ, L.C.S. performed the recordings in the main olfactory epithelium, J.T. performed the recordings in the olfactory bulb, M.L. supervised the bulb recordings, and M.M. supervised the whole project and drafted the manuscript.

COMPETING INTERESTS STATEMENT

The authors declare that they have no competing financial interests.

active sniffing, is necessary for olfactory perception and affects both odorant intensity and identity perception[13].

Pressure, such as that caused by airflow in the nostril, is a basic stimulus that can induce mechanical responses in various cell types. Mechanosensitivity is mediated by diverse molecular and cellular mechanisms involving surface processes (for example, cilia), subcellular structures (for example, microfilaments and microtubules) and membrane proteins (for example, ion channels and surface receptors)[14]. Membrane protein–mediated mechanotransduction, resulting either from direct opening of ion channels or from their indirect activation via second messengers, can provide key sensory information to cells[15].

We show here that individual OSNs detect two distinct sensory modalities transmitted by chemical and mechanical stimuli. Both odorant and mechanical responses are eliminated by blocking adenylyl cyclase activity or knocking out the CNG channel CNGA2 (in the *Cnga2*$^{-/y}$ mouse)[16], suggesting that both responses are mediated by a shared second-messenger cascade. We show that the mechanosensitivity enhances the neuronal activity of individual OSNs when they are weakly stimulated by odorants. Furthermore, the mechanosensitivity of the OSNs may provide a peripheral driving force to synchronize the rhythmic activity (theta-band oscillation) in the olfactory bulb with respiration, because the spontaneous theta oscillation in the bulb uncouples from respiration in *Cnga2*$^{-/y}$ mice. Taken together, these results suggest the OSNs ensure that both odor and airflow information reach the olfactory bulb by means of the chemical and mechanical sensitivities, as well as providing a driving force to synchronize the bulb activity with breathing cycles.

RESULTS

Septal organ OSNs show chemical and mechanical responses

We initially investigated the odorant response properties shown by septal organ neurons located within a small island of olfactory neuroepithelium situated in the air path of the nose[17]. The septal organ was visually identified based on its discrete location and appearance[18]. Using the perforated patch-clamp technique, we recorded odorant-induced transduction currents and receptor potentials from individual dendritic knobs of the OSNs in the intact olfactory epithelium (Fig. 1a). Odorant stimulation was delivered by a pressure ejection (puff) of odorant solutions through a multibarrel pipette, with one barrel filled with pure Ringer solution to serve as a control.

Odor puffs elicited inward currents in voltage-clamp mode in approximately 70% of the septal organ neurons (184 of 258). The response of a single neuron induced by puffing mix 1 (consisting of 100 μM of each odorant; see Methods) is shown (Fig. 1b, black trace). However, puffing Ringer solution alone also generated an inward current in the same neuron (Fig. 1b, gray trace). This result raised the possibility that these neurons responded to the mechanical stimulus delivered by puffing *per se*. To test this, we positioned the puffing pipette farther away (70 μm instead of 20 μm) so that the odorant solution diffused to the recorded cell without the pressure component. In this configuration, a response was still induced by the odor puff, but not by the Ringer puff (Fig. 1c). Whether the puffing pipette was positioned close (d = 20 μm) or far away (d = 70 μm), mix 1 always elicited bigger responses than Ringer ($P < 0.01$, n = 9; Fig. 1d). Furthermore, mix 1 stimulus from a farther distance always induced smaller responses than from a closer distance ($P < 0.01$), presumably because there was no mechanical component and a lower odor concentration reached the cell.

Because the stimulus puffs generated from different barrels within a multibarrel pipette might not be uniform, we made the following measurements to define a positive odor response. The amplitudes of Ringer puff–induced responses from various barrels of a multibarrel pipette filled

only with Ringer solution were normalized to the mean obtained from individual neurons. The frequency distribution of 56 responses from 13 neurons was fitted with a Gaussian distribution (Fig. 1e). At a 95% confidence level, a positive odor response was then defined as a response amplitude exceeding 60% of a Ringer response (mean + 2 × s.d.). A pure odor response of a neuron was obtained by one of the following two methods: subtracting the mechanical component induced by a Ringer puff from the response induced by an odor puff at the same pressure, or positioning the puffing pipette farther from the knob to eliminate the mechanical response.

The odor-responsive neurons in the septal organ (70%, $n = 258$ tested) generally responded to multiple odorants with distinct structures. For example, the neuron shown in Figure 2a responded to acetophenone, amyl acetate and benzaldehyde but not to (+)-limonene. Approximately 25% of the septal organ neurons did not respond to either odor or Ringer solution puffs delivered at the same pressure, although they did respond to a cocktail of 10 μM forskolin (an adenylyl cyclase inhibitor) and 100 μM 3-isobutyl-1-methylxanthine (IBMX, a phosphodiesterase inhibitor), indicating that the cAMP cascade was intact (Fig. 2b). These neurons also showed normal resting potentials (−60 to −70 mV) and voltage-gated ionic currents, and fired spontaneously or with current injection (Fig. 2c,d). Another 5% of the neurons responded to Ringer or odor puffs with a similar magnitude, suggesting that they underwent only the mechanical response, though the possibility exists that ineffective ligands were tested.

Odor-induced responses in the septal organ neurons increased with odor concentration (Fig. 2e). At concentrations of and below 10^{-10} M, octanoic acid elicited responses similar to those induced by puffing Ringer alone (gray trace). At concentrations of 10^{-8} M and above, octanoic acid elicited responses that increased with concentration. Dose-response relations based on the peak currents from four neurons are shown (Fig. 2f). For each neuron, there was a non-zero baseline response ($I_{baseline}$) elicited by very low concentrations (below 10^{-10} M), which was presumably the mechanical response induced by puffing *per se*.

Mechanosensitivity is widespread in OSNs

The mechanical responsiveness of the OSNs was further confirmed by experiments involving a single-barrel pipette filled only with Ringer solution (the same solution continuously perfused in the recording chamber) to provide the mechanical stimulus through pressure ejection. Such design negated any possible odorant contamination from other barrels within a multibarrel pipette and any difference between solutions (such as osmolarity, temperature or pH; see Methods). Of the 46 septal organ neurons tested with a single-barrel pipette filled with Ringer, 33 (76.7%) responded to Ringer puffs (Fig. 3a).

Because this mechanical responsiveness was relatively common in the septal organ neurons, we next asked whether the same sensitivity existed in the main olfactory epithelium. We examined OSNs from different regions in the main epithelium: 19 from the most ventral zone and 18 from the most dorsal zone. One neuron in the main olfactory epithelium that responded to Ringer puffs is shown (Fig. 3b). In total, 49% of the neurons (18 of 37) responded to Ringer puffs alone and there was no difference in the responses from different zones. The results indicate that the mechanosensitivity is a ubiquitous feature in both the septal organ and the main olfactory epithelium.

For all neurons tested with different pressures, the peak amplitudes of the responses increased with pressure (Fig. 3a,b). Because we did not observe significant differences in the response-pressure relations between the septal organ and the main olfactory epithelium neurons, we summarized the response-pressure relations from four neurons in each region together. For each neuron, the peak currents induced by different pressures (x) were normalized to the

saturating response obtained from the Boltzmann equation fitting (close to that induced by 50 p.s.i.). The data at each pressure point were then averaged from all eight neurons (I_{mean}) and fitted by the Boltzmann equation $I_{mean} = I_{max} - I_{max}/(1 + e^{(x-x0)/dx})$, with the maximum I_{max} = 0.98, the center x_0 = 15.9 p.s.i. and the time constant dx = 7.3 (Fig. 3c). The pressures used in this study are within the physiological range for normal breathing and sniffing (see Discussion).

The mechanical responses are mediated by a cAMP cascade

To determine the mechanism underlying the mechanosensitivity of the OSNs, the reversal potential of the responses was obtained by recording Ringer-induced currents at different holding potentials (−60 mV to + 40 mV) (n = 4, the septal organ) (Fig. 3d,e). Much as with the odorant responses, the polarity of the pressure-induced currents reversed at around 0 mV, indicating the currents were carried by nonspecific cation channels. In addition, upon stimulation at 20 p.s.i., the mechanical responses of the septal organ neurons showed a relatively long latency (defined as the time from onset of the pulse to start of the response) of 333 ± 25 ms (n = 32), which was significantly longer than that induced by 10 μM mix 1 (225 ± 25 ms, n = 24; $P < 0.001$ in t-test). The latency became shorter with higher pressures in some cells (Fig. 3a), but the averaged latency at 40 p.s.i. was not significantly shorter than that at 20 p.s.i. Furthermore, the decay phase of the mechanical responses resembled that induced by odorants: that is, the responses reached the peak and started to decline before offset of the stimulus (Fig. 3a,**b**). When the decay phase was approximately fitted to a single exponential curve, the mechanical responses of the septal organ neurons (stimulated at 20 p.s.i.) generated an averaged time constant of 0.7 s (±0.1 s, n = 32). The response latency and kinetics suggest that the mechanical response is mediated through a second-messenger pathway rather than through the direct opening of an ion channel.

We then tested a pharmacological blocker of the odorant responses for its possible interference with the mechanical responses. An adenylyl cyclase blocker, 50 μM MDL12330A, which inhibited odorant responses in OSNs[19,20], reversibly blocked the mechanical responses (Fig. 4a, n = 5). In addition, odorant responses become larger and longer-lasting in Ca^{2+}-free solutions, presumably as a result of the removal of Ca^{2+}-mediated inhibition of the CNG channels[21,22]. The mechanical responses in Ca^{2+}-free solution mirrored the behavior of the odor-induced responses (Fig. 4b, n = 4).

Furthermore, Ca^{2+}-mediated inhibition of the CNG channels underlies odor adaptation during repeated stimuli: that is, the first stimulus typically elicits a bigger response than do subsequent ones[23]. We examined whether the mechanical responses underwent adaptation during repetitive Ringer puffs. The septal organ neurons followed Ringer puff frequencies of up to 0.5 Hz and showed adaptation in both voltage- and current-clamp modes (Fig. 4c,**d**). When the stimuli were presented at higher frequencies, for instance at 1 Hz, the neurons responded to every other pulse so that the response frequency remained at ~ 0.5 Hz (Fig. 4e).

Finally, we tested the existence of the mechanical responses in male *Cnga2*-null (*Cnga2*$^{-/y}$) mice. None of the 18 neurons from these mice tested in the septal organ responded to either odorant or Ringer puffs, even though these neurons had normal resting potentials (−60 to −70 mV) and voltage-gated ionic currents, and fired action potentials (Fig. 4f–h). Overall, these results indicate that the mechanical responses are mediated by a second-messenger cascade involving cAMP and the CNG channels.

OSNs sense airflow information via mechanosensitivity

We hypothesize that the mechanical sensitivity of the OSNs serves at least two functions. First, it might enhance the odorant responses of individual neurons when the airflow increases in the

nostrils such as during sniffing[13]. Because some OSNs respond to both odorant and mechanical stimuli, integration of these two components becomes possible at the single-cell level. To test this, we examined the responses of individual septal organ neurons to the same odorant delivered with different pressures. The responses to 1 μM octanoic acid (a relatively weak stimulus) in a single neuron increased with the ejection pressure (Fig. 5a; $n = 4$). We used pressures above 20 p.s.i. because junction potential measurements (see Methods) showed that the odor concentration reaching the recording site remained constant above this pressure. The increased responses observed here were presumably due to an increase in the mechanical component elicited under higher pressures.

The mechanical responses showed more significant effects on neuronal activity when the neurons were weakly as compared to strongly stimulated with odorants. The transduction currents induced by saturating odorants (100 μM mix 1) showed less augmentation with increasing pressures than did those elicited by 1 μM octanoic acid (Fig. 5b; $n = 4$). This became more obvious in current-clamp mode when the firing frequency was measured. Figure 5c shows the receptor potentials and action potentials induced by 1 μM octanoic acid under different pressures in a septal organ neuron. The averaged firing frequencies were measured from the onset of the response to the end of the first major burst for each trace (rectangle in Fig. 5c). The firing frequencies increased with the delivery pressure for weak stimuli (1 μM octanoic acid, $n = 5$) but not for strong stimuli ($n = 4$) (Fig. 5d). Presumably the firing rate was nearly saturated with strong stimulation. These results suggest that the mechanical response can increase the firing frequency of individual neurons, especially when induced by weak odor stimuli.

The second possible function afforded by the mechanosensitivity of the OSNs is a peripheral drive to synchronize the rhythmic activity (theta oscillation) in the olfactory bulb with respiration. Because the mechanical sensitivity of the sensory neurons was eliminated in *Cnga2*$^{-/y}$ mice, we predicted that we would observe uncoupling of the bulb activity and respiration in these animals. To test this, field potential recordings were performed in the olfactory bulb of both wild-type and *Cnga2*$^{-/y}$ mice. Five penetrations were made on the dorsal surface of each bulb and the field potentials were recorded at four depths: 100, 200, 330 and 500 μm. In wild-type mice, the rhythmic activity was coupled to respiration at all depths but with different depth-dependent time lags, which were evident in the averaged field potentials (Fig. 6a,**b**). In contrast, the *Cnga2*$^{-/y}$ bulbs showed a slower rhythmic activity, which completely uncoupled from respiration at all recording depths (Fig. 6c,**d**). We then compared the cross-correlation coefficients between the field potentials and respiration cycles in wild-type ($n = 6$) and *Cnga2*$^{-/y}$ bulbs ($n = 4$). For each bulb, the coefficients at each depth were averaged from the five penetrations. The averaged coefficients at all depths were significantly lower for *Cnga2*$^{-/y}$ mice than for wild-type mice, as demonstrated by the two examples at depths of 100 μm and 500 μm (Fig. 6e). These data strongly indicate that the OSNs provide the peripheral driving force to synchronize the oscillatory activity in the bulb with the breathing cycles. The ability of the relatively slow mechanical responses (Fig. 4c–e) to drive the rhythmic activity in the bulb during fast breathing cycles is discussed later.

DISCUSSION

Using patch-clamp recordings from individual neurons, we discovered that many OSNs can sense two distinct modalities transmitted by chemical and mechanical stimuli. In addition, the odorant and mechanical responses of the OSNs are most likely mediated by a shared second-messenger pathway involving cAMP and the CNG channels. Furthermore, the mechanical responses enhance the neuronal activity of individual OSNs when these are weakly stimulated by odorants. Finally, the mechanosensitivity of the OSNs may provide a peripheral driving force to synchronize the olfactory bulb activity (theta oscillation) with the breathing cycles.

Many septal organ neurons respond not only to odorants, but also to pure mechanical stimuli induced by puffs of odor-free Ringer solution (Fig. 1). Therefore, a response induced by an odor puff sums the odorant and mechanical components. Because the mechanical responses induced by different barrels are similar (Fig. 1e), the larger responses induced by higher-concentration applications should result from stronger odor stimulation (Fig. 2e,**f**). The mechanical responses observed here are unlikely to be recording artifacts, especially because the neurons responded to alternate pulses when they were stimulated at 1 Hz (Fig. 4e). Notably, the mechanical sensitivity is not unique to the septal organ neurons, as it also exists in nearly 50% of the neurons in the main olfactory epithelium (Fig. 3b).

The mechanical responses of OSNs are likely to be mediated by a second-messenger pathway involving cAMP and the CNG channels. The responses occur with relatively long delays and are completely blocked by an inhibitor of adenylyl cyclase, suggesting that cAMP is involved as a second messenger. Elimination of mechanosensitivity in the OSNs from *Cnga2*$^{-/y}$ mice further supports this notion. In the mouse OSNs, it remains to be determined what upstream steps, including which receptors and G proteins, are involved in the cAMP-mediated mechanosensitivity. One possibility is that some odorant receptors are sensitive to pressure, much like another G protein–coupled receptor, the NMDA receptor[24]. Alternatively, a mechanosensor in the membrane might cross-link to the cAMP cascade.

One possible role of the mechanosensitivity of the OSNs is implied by its interaction with odorant responses. When the air flows faster in the nose, for instance during sniffing, the observed mechanosensitivity may make neurons more likely to fire (Fig. 5). This will increase the overall sensitivity of the olfactory system, especially when it is weakly stimulated. Indeed, psychophysical studies indicate that the sniff volume is inversely proportional to odor concentrations[25,26]. Integration of respiration (airflow) with odor-induced responses in the olfactory system is essential for the brain to decipher odor quality and intensity perceived by the peripheral organ[13].

To determine whether the pressures we delivered to the neurons were within the physiological range of normal breathing or sniffing, we have made the following estimate. Consider a 20-p.s.i. pressure that is delivered to a puffing pipette tip without any leak along the tubes. The opening of each barrel is calculated as 4 μm in diameter on the basis of the size of the tip and the outside and inside diameters of the glass. During a 1-s puff, the food color used to indicate the stimulus (see Methods) forms a ‘cone’ with a diameter of 50 μm at the recording site. The pressure at this point is then estimated to be $20 \times 4^2/50^2 = 0.12$ p.s.i. Assuming the animal breathes at a frequency (f) of 6 Hz with a tidal volume (V_t) of 0.2 ml and an airway resistance (R_{aw}) of 2.3 $cmH_2O \cdot ml^{-1}s$ (ref. 27), the pressure drops (ΔP) in the airway can be calculated as $\Delta P = R_{aw} \times f \times V_t = 2.76$ cmH_2O, or 0.04 p.s.i. Considering that the septal organ neurons responded to a delivery pressure of 2 p.s.i. (equivalent to 0.012 p.s.i. at the recording site) and the airflow in the nostril would be higher during sniffing, the pressures we used here should be relevant under physiological conditions.

A second possible role of OSN mechanosensitivity may be to synchronize the rhythmic activity in the olfactory bulb with the breathing cycles. In *Cnga2*$^{-/y}$ mice, the OSNs do not show mechanical responses, and the rhythmic activity in the bulb uncouples from respiration (Figs. 4 and **6**). The residual oscillation observed in *Cnga2*$^{-/y}$ mice is presumably due to the intrinsic properties of the bulb circuits[28–32]. We cannot completely rule out the possibility that other deficits in *Cnga2*$^{-/y}$ cause the effect. However, given that the rhythmic activity was recorded in the absence of odorants (Fig. 6) and the OSNs in the knockout mice were capable of firing action potentials (Fig. 4h), it is plausible that uncoupling of the bulb activity from respiration results from lack of the mechanosensitivity in the OSNs. The results strongly support the idea that the OSNs provide the driving force for such synchronization. Consistent with our findings,

tracheo-tomization and naris closure also cause uncoupling of the bulb activity from respiration[4,6,7]. Therefore, the mechanosensitivity of the OSNs, in addition to episodic access to odorants, may cause the respiration-coupled, odorant-induced activity in the olfactory epithelium[33], the olfactory bulb[5,6,34–36] and the olfactory cortex[4].

The mechanical response of a single neuron follows a maximum frequency of only 0.5 Hz (Fig. 4c–e), which is notably slower than normal breathing. However, by converging the mechanical inputs of a few thousand neurons, the corresponding glomerular units within the bulb might show rhythmic activity that follows respiration, even if only a fraction of the neurons respond in each cycle. The mechanical sensitivity exists in many but not all sensory neurons (70% in the septal organ and 50% in the main olfactory epithelium), which may explain why rhythmic activity in the absence of odorants has been observed in some neurons of the olfactory bulb in certain studies[6] but not in others[12].

Our work reveals that the mammalian OSNs can serve dual functions as odor detectors and mechanical sensors, which seem to be mediated by shared cellular mechanisms. Integration of the chemical and mechanical responses in the OSNs and direct delivery of the airflow information to the olfactory bulb add a new dimension for sensory coding in the mammalian olfactory system.

METHODS

Epithelial preparations

The intact epithelial preparations were prepared following published procedures37,38. Wild-type (male or female, 3–12 weeks of age) or *Cnga2*$^{-/y}$ (male, 12 weeks of age) mice16 were deeply anesthetized by injection of ketamine and decapitated. The head of each mouse was immediately put into ice-cold Ringer solution, which contained 124 mM NaCl, 3 mM KCl, 1.3 mM $MgSO_4$, 2 mM $CaCl_2$, 26 mM $NaHCO_3$, 1.25 mM NaH_2PO_4, 15 mM glucose, pH 7.6 and 305 mOsm. The pH was kept at 7.4 after bubbling of the solution with 95%O_2/5%CO_2. The nose was dissected out *en bloc* and kept in oxygenated Ringer solution. Before use, the entire epithelium attached to the nasal septum was peeled away from the underlying bone and transferred to a recording chamber. Oxygenated Ringer was continuously perfused at 25 ± 2 ° C. Ca^{2+}-free solution contained 124 mM NaCl, 3 mM KCl, 1.3 mM $MgSO_4$, 26 mM $NaHCO_3$, 1.25 mM NaH_2PO_4, 15 mM glucose, 3 mM EGTA, pH 7.6 and 305 mOsm. The animal handling procedure were approved by the institutional animal care and use committee of the University of Pennsylvania.

Patch clamp

The dendritic knobs of the OSNs were visualized through an upright differential interference contrast (DIC) microscope (Olympus BX51WI) equipped with a CCD camera (Dage-MTI) and a 40× water-immersion objective. An extra 4× magnification was achieved by an accessory lens in the light path. Electrophysiological recordings were controlled by an EPC-10 amplifier combined with Pulse software (HEKA Electronic). Perforated patch clamping was performed on the dendritic knobs by including 260 μM nystatin in the recording pipette, which was filled with the following solution: 70 mM KCl, 53 mM KOH, 30 mM methanesulfonic acid, 5.0 mM EGTA, 10 mM HEPES, 70 mM sucrose; pH 7.2 (KOH) and 310 mOsm. The junction potential was approximately 9 mV and was corrected in all experiments within the software.

A multibarrel pipette, placed 20 μm downstream from the recording site (if not otherwise stated), was used to deliver stimuli by pressure ejection through a picospritzer (Pressure System IIe). All stimuli were delivered at 20 p.s.i. (138 kPa, unless otherwise stated) with a pulse length of 0.5–1 s to ensure that the cells were essentially stimulated by the concentration included in

the puffing pipettes, based on the following two controls39. In the first control, a recording electrode filled with Ringer was used to measure the junction potentials induced by 3 M KCl solution included in the puffing pipettes. The junction potential plateau increased with the pressure from 5 to 20 p.s.i. and stayed constant above 20 p.s.i. At all pressures, the junction potentials reached the maximum value with pulses ≥300 ms. In the second control, the light intensity changes caused by puffing food colors (0.05–2 s) were used as an indication of the odor 'concentration' in the recording chamber and a maximum plateau was reached with pulses ≥300 ms.

The pH level of the perfused Ringer was kept constant at 7.4 by bubbling with 95%O_2/5% CO_2, whereas the solution in the puffing pipette was not bubbled. To rule out the possibility that the responses to Ringer puffs were caused by pH difference in the solutions, the puffing pipettes were filled with the bubbled solution and used within 4 h, during which time the pH changes were minimal (within 0.2). In another set of control experiments, seven-barrel pipettes were filled with Ringer solution adjusted to different pH levels (6.0–10.0) using HCl or NaOH. The responses induced by the solutions of different pH were similar (n = 4, data not shown).

Odorants

Odorants were prepared as 0.5 M solutions in dimethyl sulfoxide (DMSO) and kept at −20 °C. IBMX was prepared as a 20 mM stock solution containing 20% DMSO. Forskolin and MDL12330A were prepared in DMSO at 10 and 13.3 mM, respectively. Final solutions were made before each experiment by adding Ringer solution. The odor mixture (mix 1) contained 19 compounds: heptanol, octanol, hexanal, heptanal, octanal, heptanoic acid, octanoic acid, cineole, amyl acetate, (+)-limonene, (−)-limonene, (+)-carvone, (−)-carvone, 2-heptatone, anisaldehyde, benzaldehyde, acetophenone, 3-hepta-none and ethyl vanilline. All compounds and chemicals were obtained from Sigma-Aldrich.

Olfactory bulb recordings

Wild-type or *Cnga2*$^{-/y}$ mice (8–12 weeks of age) were anesthetized with ketamine and xylazine. Air filtered with active charcoal was continuously applied through Teflon tubing with the opening 1 cm away from the nostrils (1 liter per min). Part of the skull was removed to expose the olfactory bulb. Glass pipettes filled with 1 M NaCl (2–5 MΩ) were used to record local field potentials in the olfactory bulb (0.5–100 Hz). The animal's respiratory rhythm was simultaneously monitored by attaching a strain gage to the chest skin. The signals were recorded through AxonClamp 2B and Brownlee 440 amplifiers. Programs for data acquisition and analysis were written in Visual Basic and Matlab, respectively.

Acknowledgements

This work was supported by the US National Institutes of Health (National Institute on Deafness and Other Communication Disorders), the Whitehall Foundation and the University of Pennsylvania Institute on Aging (a pilot grant). We thank H. Zhao at Johns Hopkins University for providing the *Cnga2* knockout mice and A. Gelperin, P. Haydon and M. Nusbaum for insightful discussions.

References

1. Buck L, Axel R. A novel multigene family may encode odorant receptors: a molecular basis for odor recognition. Cell 1991;65:175–187. [PubMed: 1840504]
2. Firestein S. How the olfactory system makes sense of scents. Nature 2001;413:211–218. [PubMed: 11557990]
3. Adrian ED. The role of air movement in olfactory stimulation. J Physiol (Lond) 1951;114:4–5p. [PubMed: 14861801]

4. Fontanini A, Spano P, Bower JM. Ketamine-xylazine-induced slow (< 1.5 Hz) oscillations in the rat piriform (olfactory) cortex are functionally correlated with respiration. J Neurosci 2003;23:7993–8001. [PubMed: 12954860]
5. Macrides F, Chorover SL. Olfactory bulb units: activity correlated with inhalation cycles and odor quality. Science 1972;175:84–87. [PubMed: 5008584]
6. Onoda N, Mori K. Depth distribution of temporal firing patterns in olfactory bulb related to air-intake cycles. J Neurophysiol 1980;44:29–39. [PubMed: 7420137]
7. Philpot BD, Foster TC, Brunjes PC. Mitral/tufted cell activity is attenuated and becomes uncoupled from respiration following naris closure. J Neurobiol 1997;33:374–386. [PubMed: 9322155]
8. Ueki S, Domino EF. Some evidence for a mechanical receptor in olfactory function. J Neurophysiol 1961;24:12–25. [PubMed: 13778965]
9. Potter H, Chorover SL. Response plasticity in hamster olfactory bulb: peripheral and central processes. Brain Res 1976;116:417–429. [PubMed: 974785]
10. Ravel N, Caille D, Pager J. A centrifugal respiratory modulation of olfactory bulb unit activity: a study on acute rat preparation. Exp Brain Res 1987;65:623–628. [PubMed: 3556489]
11. Ravel N, Pager J. Respiratory patterning of the rat olfactory bulb unit activity: nasal versus tracheal breathing. Neurosci Lett 1990;115:213–218. [PubMed: 2234500]
12. Sobel EC, Tank DW. Timing of odor stimulation does not alter patterning of olfactory bulb unit activity in freely breathing rats. J Neurophysiol 1993;69:1331–1337. [PubMed: 8492167]
13. Mainland J, Sobel N. The sniff is part of the olfactory percept. Chem Senses 2005;31:181–196. [PubMed: 16339268]
14. Ingber DE. Cellular mechanotransduction: putting all the pieces together again. FASEB J 2006;20:811–827. [PubMed: 16675838]
15. Lin SY, Corey DP. TRP channels in mechanosensation. Curr Opin Neurobiol 2005;15:350–357. [PubMed: 15922584]
16. Zhao H, Reed RR. X inactivation of the OCNC1 channel gene reveals a role for activity-dependent competition in the olfactory system. Cell 2001;104:651–660. [PubMed: 11257220]
17. Rodolfo-Masera T. Su 1'esistenza di un particolare organo olfacttivo nel setto nasale della cavia e di altri roditori. Arch Ital Anat Embryol 1943;48:157–212.
18. Ma M, et al. Olfactory signal transduction in the mouse septal organ. J Neurosci 2003;23:317–324. [PubMed: 12514230]
19. Chen S, Lane AP, Bock R, Leinders-Zufall T, Zufall F. Blocking adenylyl cyclase inhibits olfactory generator currents induced by "IP(3)-odors". J Neurophysiol 2000;84:575–580. [PubMed: 10899229]
20. Spehr M, Wetzel CH, Hatt H, Ache BW. 3-phosphoinositides modulate cyclic nucleotide signaling in olfactory receptor neurons. Neuron 2002;33:731–739. [PubMed: 11879650]
21. Kurahashi T, Shibuya T. Ca^{2+}-dependent adaptive properties in the solitary olfactory receptor cell of the newt. Brain Res 1990;515:261–268. [PubMed: 2113412]
22. Zufall F, Shepherd GM, Firestein S. Inhibition of the olfactory cyclic nucleotide gated ion channel by intracellular calcium. Proc R Soc Lond B 1991;246:225–230.
23. Zufall F, Leinders-Zufall T. The cellular and molecular basis of odor adaptation. Chem Senses 2000;25:473–481. [PubMed: 10944513]
24. Paoletti P, Ascher P. Mechanosensitivity of NMDA receptors in cultured mouse central neurons. Neuron 1994;13:645–655. [PubMed: 7917295]
25. Johnson BN, Mainland JD, Sobel N. Rapid olfactory processing implicates subcortical control of an olfactomotor system. J Neurophysiol 2003;90:1084–1094. [PubMed: 12711718]
26. Laing DG. Natural sniffing gives optimum odour perception for humans. Perception 1983;12:99–117. [PubMed: 6657430]
27. Lai-Fook SJ, Lai YL. Airway resistance due to alveolar gas compression measured by barometric plethysmography in mice. J Appl Physiol 2005;98:2204–2218. [PubMed: 15677740]
28. Balu R, Larimer P, Strowbridge BW. Phasic stimuli evoke precisely timed spikes in intermittently discharging mitral cells. J Neurophysiol 2004;92:743–753. [PubMed: 15277594]

29. Hayar A, Karnup S, Shipley MT, Ennis M. Olfactory bulb glomeruli: external tufted cells intrinsically burst at theta frequency and are entrained by patterned olfactory input. J Neurosci 2004;24:1190–1199. [PubMed: 14762137]

30. Hayar A, Shipley MT, Ennis M. Olfactory bulb external tufted cells are synchronized by multiple intraglomerular mechanisms. J Neurosci 2005;25:8197–8208. [PubMed: 16148227]

31. Schoppa NE, Westbrook GL. Glomerulus-specific synchronization of mitral cells in the olfactory bulb. Neuron 2001;31:639–651. [PubMed: 11545722]

32. Urban NN, Sakmann B. Reciprocal intraglomerular excitation and intra- and interglomerular lateral inhibition between mouse olfactory bulb mitral cells. J Physiol (Lond) 2002;542:355–367. [PubMed: 12122137]

33. Chaput MA. EOG responses in anesthetized freely breathing rats. Chem Senses 2000;25:695–701. [PubMed: 11114147]

34. Cang J, Isaacson JS. *In vivo* whole-cell recording of odor-evoked synaptic transmission in the rat olfactory bulb. J Neurosci 2003;23:4108–4116. [PubMed: 12764098]

35. Luo M, Katz LC. Response correlation maps of neurons in the mammalian olfactory bulb. Neuron 2001;32:1165–1179. [PubMed: 11754845]

36. Spors H, Wachowiak M, Cohen LB, Friedrich RW. Temporal dynamics and latency patterns of receptor neuron input to the olfactory bulb. J Neurosci 2006;26:1247–1259. [PubMed: 16436612]

37. Ma M, Chen WR, Shepherd GM. Electrophysiological characterization of rat and mouse olfactory receptor neurons from an intact epithelial preparation. J Neurosci Methods 1999;92:31–40. [PubMed: 10595701]

38. Ma M, Shepherd GM. Functional mosaic organization of mouse olfactory receptor neurons. Proc Natl Acad Sci USA 2000;97:12869–12874. [PubMed: 11050155]

39. Grosmaitre X, Vassalli A, Mombaerts P, Shepherd GM, Ma M. Odorant responses of olfactory sensory neurons expressing the odorant receptor MOR23: a patch clamp analysis in gene-targeted mice. Proc Natl Acad Sci USA 2006;103:1970–1975. [PubMed: 16446455]

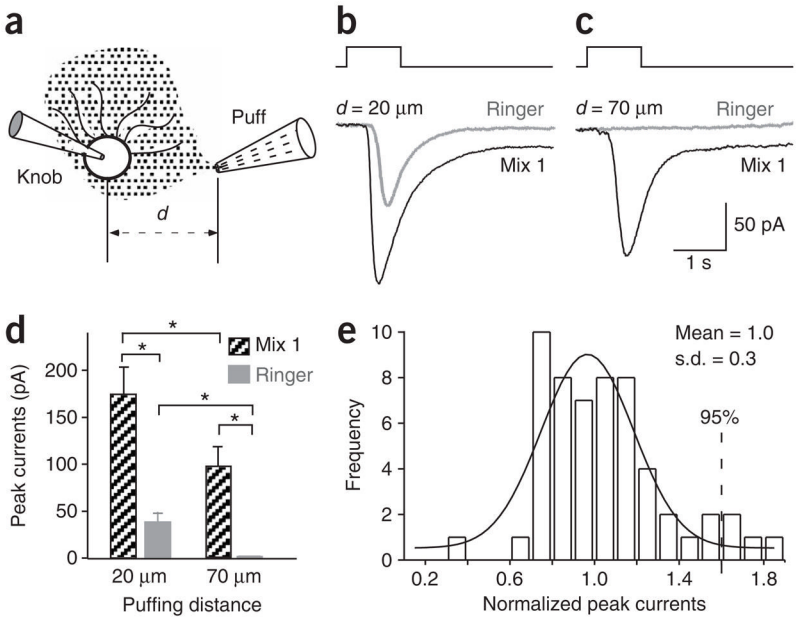

Figure 1.

The septal organ neurons respond to both chemical and mechanical stimuli. (**a**) Schematic drawing shows the recording configuration. The distance between the recorded knob and the puffing pipette opening is defined as the puffing distance (*d*). (**b**,**c**) In voltage-clamp mode, inward currents were elicited by mix 1 (100 μM) and Ringer solution puffs from a single neuron with the puffing distance *d* =20 μm (**b**) or 70 μm (**c**). The holding potential was −60 mV. (**d**) The peak currents induced by mix 1 or Ringer puffs are averaged from nine neurons. Star (*) marks significant difference in paired *t*-test ($P < 0.01$). (**e**) The responses induced by Ringer puffs show variation. The inward currents were induced by Ringer puffs via different barrels of puffing pipettes and the peak currents were normalized to the mean obtained from individual neurons. The frequency distribution is plotted with a bin width of 0.1 and fitted by a Gaussian distribution (smoothed line). The mean of the normalized peak currents is 1.0 and the s.d. is 30%. The puffing pressure was 20 p.s.i. for all recordings.

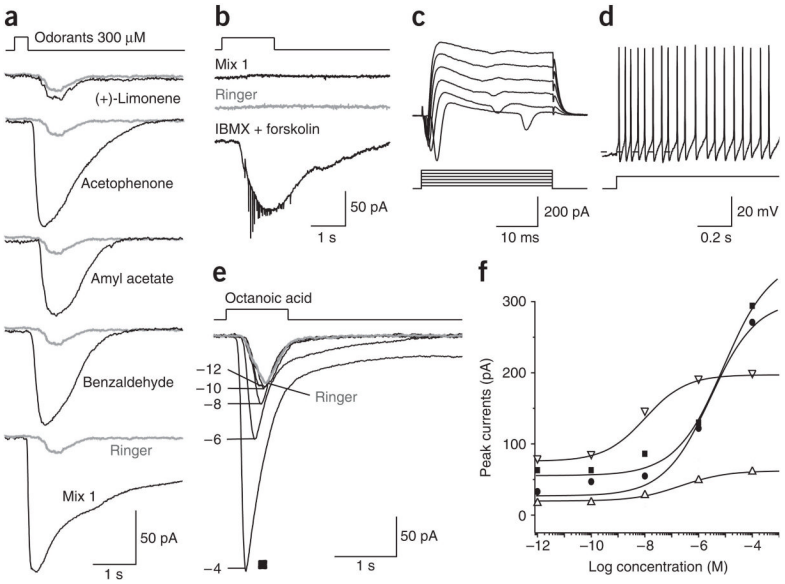

Figure 2.

The septal organ neurons respond to diverse odorants and mechanical stimulation. (**a**) A single neuron responded to multiple odorants (except (+)-limonene) at 300 μM. Inward currents were elicited by odor and Ringer solution puffs in voltage-clamp mode. The same Ringer response (gray) was shown with each odorant response. (**b–d**) A non-responsive neuron showed normal functional properties. In voltage-clamp mode, a single neuron did not respond to mix 1 (100 μM) or Ringer puffs, but responded to a cocktail of IBMX and forskolin (**b**). In the same neuron, voltage-gated ionic currents were elicited by voltage steps from −40 to +60 mV (**c**) and action potentials were elicited by injecting a depolarizing current (6 pA) (**d**). The dashed line marks −60 mV. (**e**,**f**) The septal organ neurons responded to octanoic acid with a low threshold and a wide dynamic range. (**e**) Inward currents from a single neuron (filled squares in **f**) were elicited by puffing octanoic acid at different concentrations (10^{-12}–10^{-4} M) in voltage-clamp mode. The gray trace indicates the response induced by puffing Ringer. (**f**) The dose-response curves (peak current I versus concentration C) are plotted and fitted with the modified Hill equation $I = I_{baseline} + I_{max}/(1 + (K_{1/2}/C)^n)$, where $n = 0.5 \pm 0.1$ ($n = 4$, mean ± s.e.m.) and $K_{1/2} = 3.2 \pm 2.3$ μM. The holding potential was −60 mV for all recordings in voltage-clamp mode and the puffing pressure was 20 p.s.i. for all recordings.

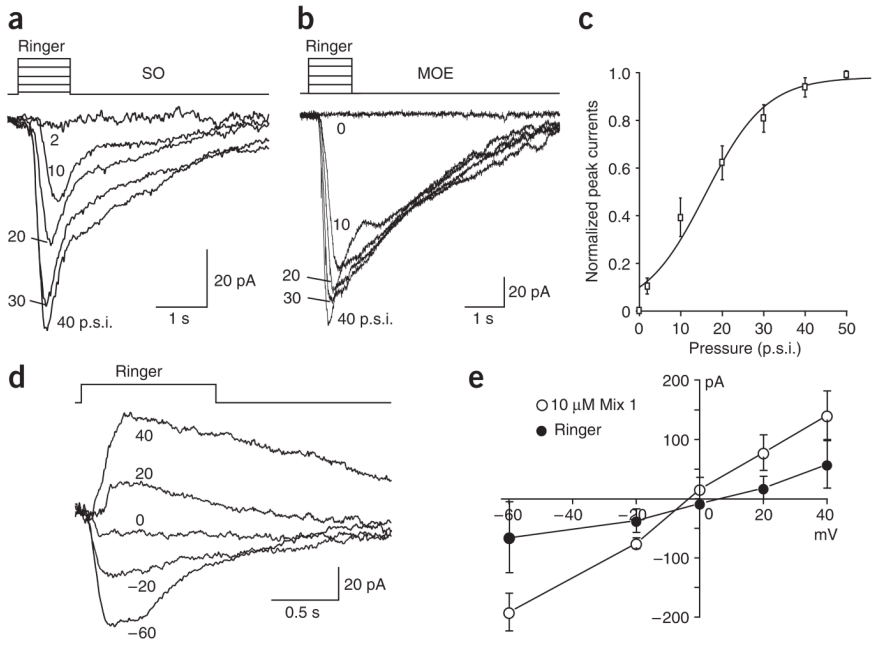

Figure 3.

OSNs from both the septal organ and the main olfactory epithelium show mechanical responses. (**a**,**b**) Inward currents from a single neuron within the septal organ (SO; **a**) or within the main olfactory epithelium (MOE; **b**) were induced by Ringer solution puffs at different pressures in p.s.i. in voltage-clamp mode. The holding potential was −60 mV for both neurons. (**c**) The normalized peak currents induced by Ringer puffs are plotted against the pressure and fitted with the Boltzmann equation. (**d**,**e**) The currents induced by Ringer puffs reversed at 0 mV in voltage-clamp mode. (**d**) The currents were induced by puffing Ringer at varying holding potentials indicated next to each trace. (**e**) The peak currents induced by mix 1 and Ringer puffs from four cells are plotted against the holding potentials. The puffing pressure was 20 p.s.i. for recordings in **d** and **e**. Error bars, s.e.m.

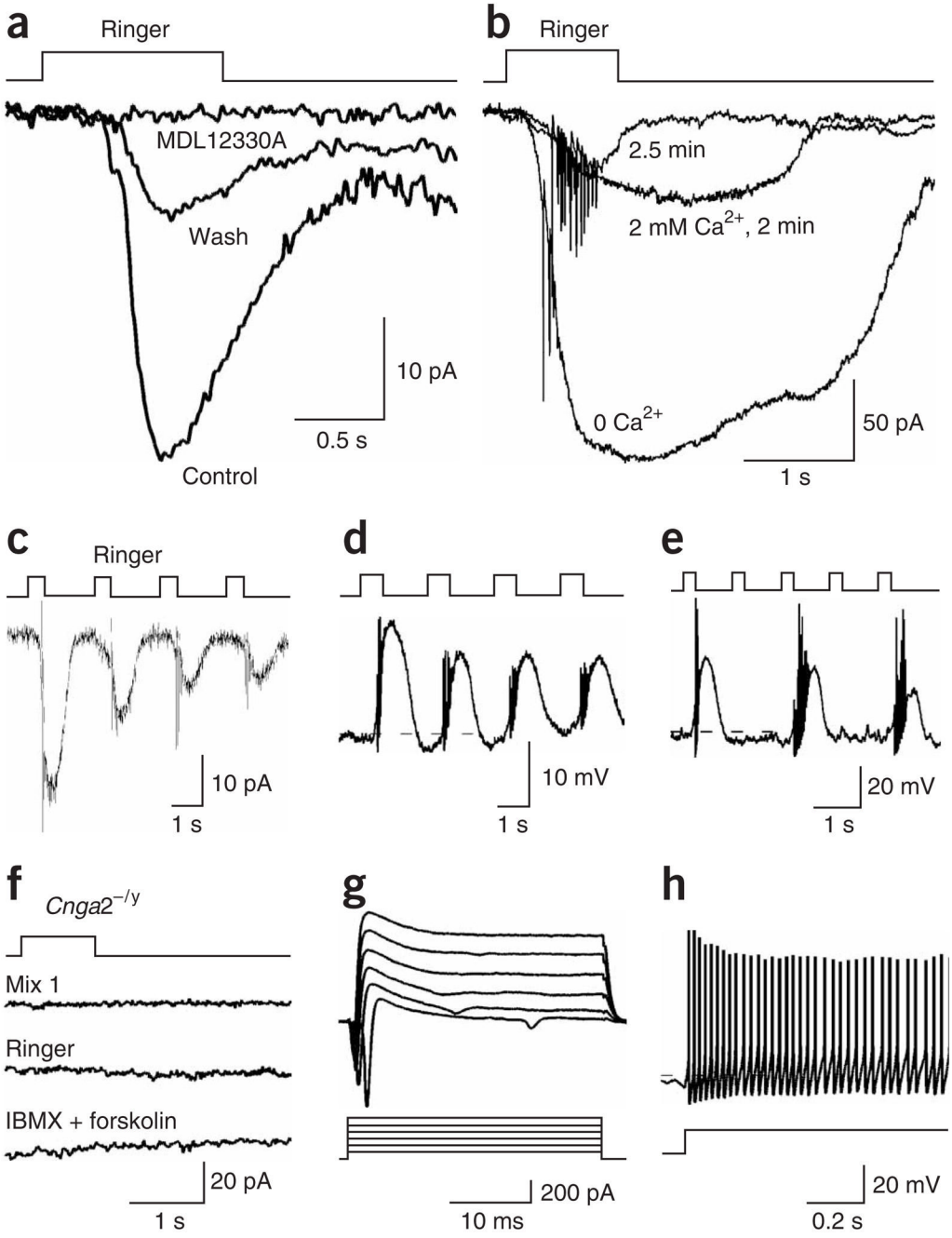

Figure 4.

The cAMP cascade and CNG channels underlie the mechanical responses of the OSNs. (**a**) The inward currents induced by Ringer solution puffs in voltage-clamp mode were reversibly blocked by 50 μM of MDL12330A, an adenylyl cyclase inhibitor. (**b**) The inward currents induced by Ringer puffs were first obtained in Ca^{2+}-free solution and then after perfusion of normal Ringer with 2 mM Ca^{2+} (2 or 2.5 min). (**c**–**e**) The mechanical responses showed adaptation during repetitive stimuli. (**c**) The inward current was induced by Ringer puffs at 0.5 Hz in voltage-clamp mode. (**d**) The depolarization was induced by Ringer puffs at 0.5 Hz in current-clamp mode. (**e**) A septal organ neuron responded to alternate Ringer puffs at 1 Hz in current-clamp mode. (**f**–**h**) Both odorant and mechanical responses were eliminated in

Cnga2$^{-/y}$ mice. (**f**) A single septal organ neuron did not respond to odorant, Ringer or IBMX +forskolin puffs in voltage-clamp mode. (**g**) In the same neuron as in **f**, voltage-gated ionic currents were elicited by voltage steps from −40 to +60 mV from a holding potential of −60 mV. (**h**) In current-clamp mode, action potentials were elicited by injecting a depolarizing current of 10 pA into the same neuron. The holding potential was −60 mV for all recordings in voltage-clamp mode. The dashed lines mark −60 mV. The puffing pressure was 20 p.s.i. for all recordings.

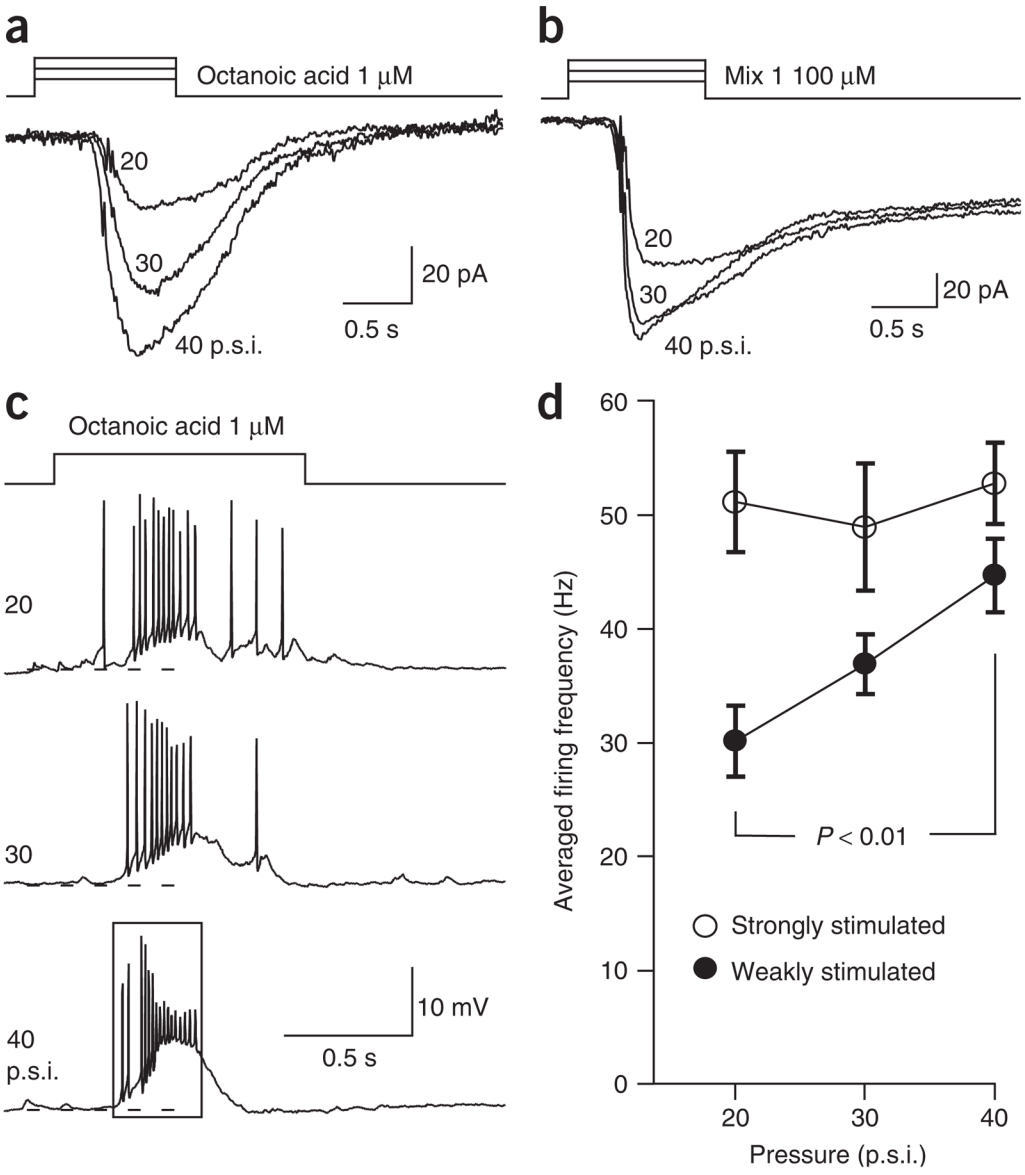

Figure 5.

Increasing puffing pressure enhances the odorant responses in individual OSNs. (**a**) In voltage-clamp mode, inward currents were induced by 1 μM octanoic acid puffs at different pressures indicated next to each trace. (**b**) Inward currents were induced by 100 μM mix 1 puffs at different pressures. The holding potential was −60 mV for both neurons. (**c**) In current-clamp mode, action potentials were elicited by 1 μM octanoic acid puffs with increasing pressures. The rectangle indicates the time window in which the firing frequency is averaged. The dashed lines mark −60 mV. (**d**) The firing frequencies are averaged for the responses induced by odorant stimuli with increasing pressures. The neurons were either 'weakly stimulated' by 1 μM octanoic acid ($n = 5$) or 'strongly stimulated' by saturating odorants (100 μM mix 1 or 300 μM octanoic acid, $n = 4$). Error bars, s.e.m.

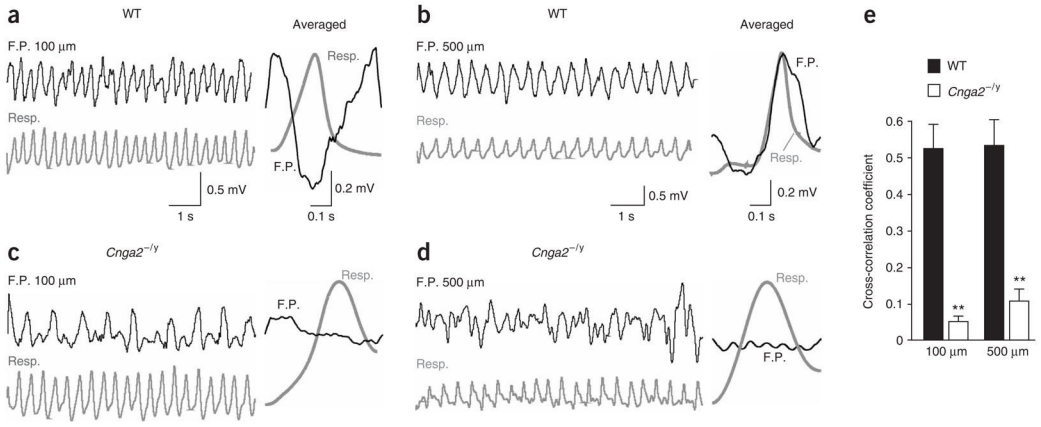

Figure 6.

The rhythmic activity (theta band) in the olfactory bulb uncouples from respiration in *Cnga2*$^{-/y}$ mice. (**a**,**b**) In wild-type (WT) olfactory bulbs, oscillatory field potentials (F.P.) (black) were recorded at 100 µm (**a**) or 500 µm (**b**). (**c**,**d**) Field potentials (black) were recorded at the depths of 100 µm (**c**) or 500 µm (**d**) in *Cnga2*$^{-/y}$ mice. Gray traces (Resp.) indicate the respiratory rhythm. The averaged field potential within one respiratory cycle is shown in the right column of each panel. To calculate the averaged traces, the field potentials within individual respiratory cycles were truncated, normalized to the same length, and then averaged over 200 s. (**e**) The cross-correlation coefficients between the field potentials and respiratory rhythms are averaged for the recordings obtained at 100 µm or 500 µm. At both depths, the coefficients are significantly higher in wild-type ($n = 6$) than in *Cnga2*$^{-/y}$ bulbs ($n = 4$) with $P < 0.001$ in *t*-test (marked by **). Error bars, s.e.m.